

Quenching of the resonance $5s(3P_1)$ state of krypton atoms in collisions with krypton and helium atoms

D.A. Zayarnyi, A.Yu. L'dov, I.V. Kholin

Abstract. The processes of collision quenching of the resonance $5s[3/2]_1^o(^3P_1)$ state of the krypton atom are studied by the absorption probe method in electron-beam-excited high-pressure He–Kr mixtures with a low content of krypton. The rate constants of plasmochemical reactions $Kr^* + Kr + He \rightarrow Kr_2^* + He$ $[(4.21 \pm 0.42) \times 10^{-33} \text{ cm}^6 \text{ s}^{-1}]$, $Kr^* + 2He \rightarrow HeKr^* + He$ $[(4.5 \pm 1.2) \times 10^{-36} \text{ cm}^6 \text{ s}^{-1}]$ and $Kr^* + He \rightarrow \text{products} + He$ $[(2.21 \pm 0.22) \times 10^{-15} \text{ cm}^3 \text{ s}^{-1}]$ are measured for the first time. The rate constants of similar reactions are refined for krypton in the metastable $5s[3/2]_2^o(^3P_2)$ state.

Keywords: inert gases, krypton, helium, argon, resonance state, collisional quenching, plasmochemistry, absorption spectroscopy.

1. Introduction

In this paper we study experimentally plasma-chemical reaction of collisional quenching processes of excited $5s$ states of krypton atoms in the high-pressure He–Kr mixtures. These experiments are, in turn, a continuation of our research on quenching processes of lower s states of heavy inert gases – xenon, neon and krypton – in their high-pressure mixtures ($p > 1$ atm) with lighter inert buffer gases (see reviews [1, 2] and references therein, as well as more recent publications [3–6]).

The present paper is devoted to the measurement of quenching rate constants of Kr atoms in the resonance $5s[3/2]_1^o(^3P_1)$ state (see Fig. 1) in dense mixtures of Kr with the buffer gas He. We have studied the practically important high-pressure mixtures with a small relative content of Kr, excited by a beam of fast electrons.

To date, the literature completely lacks the quantitative data on such processes, despite the fact that they play an important role in forming the population inversion in high-pressure lasers on atomic transitions in inert gases [7, 8] and krypton dimer lasers [9].

At high pressures ($p = 1\text{--}4$ atm), atoms in the studied states are quenched in reactions involving collisions of three and two particles:



D.A. Zayarnyi, A.Yu. L'dov, I.V. Kholin P.N. Lebedev Physics Institute, Russian Academy of Sciences, Leninsky prosp. 53, 119991 Moscow, Russia; e-mail: kholin@sci.lebedev.ru

Received 23 December 2013; revision received 20 January 2014
Kvantovaya Elektronika 44 (11) 1066–1070 (2014)
Translated by I.A. Ulitkin

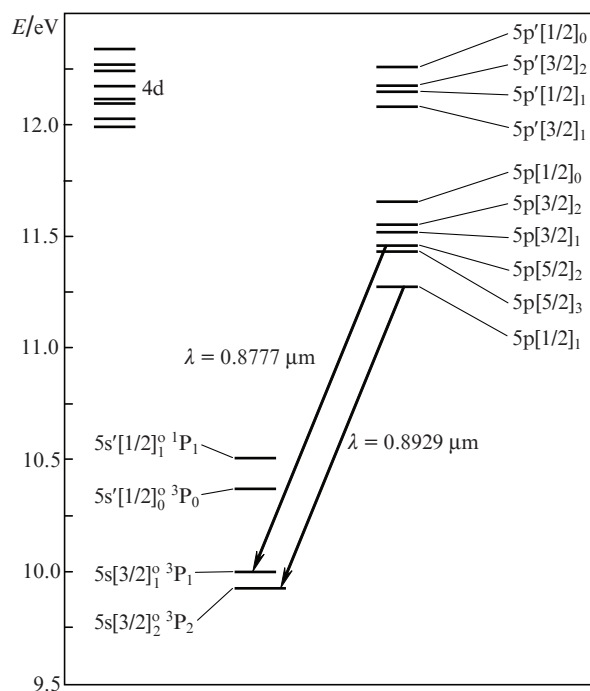
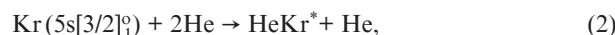


Figure 1. Diagram of the excited levels of a krypton atom.



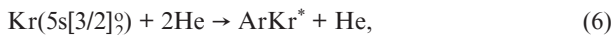
In determining the rate constant of reaction (3), we should bear in mind that the value obtained in the experiment is an upper bound, because it is also needed to take into account the reactions of excited krypton with atoms and molecules of impurities M in the gas mixture in question (mainly in He):



The relative concentrations m of different impurities M in purified He are low [6], but due to the large cross sections, the contribution of such reactions can be considerable.

For comparison, in this series of experiments we have also measured the rate constants of similar reactions for the metastable $5s[3/2]_2^o$ level, studied in our previous paper [6]





The rate constants have been measured by the absorption probe method [1, 2] from the dependence of the decay time of the states under study on the pressure and concentration ratio of the components of the working and buffer gases. To this end, in the afterglow of a high-power beam of fast electrons we have investigated the dynamics of absorption of a transmitting light pulse at a wavelength of $0.8777 \mu\text{m}$, corresponding to a high-oscillator strength optical transition between one of the upper ($5p[5/2]_2$) levels of krypton and the resonance $5s[3/2]_1^0$ level in question (see Fig. 1). As in our earlier work [6], the reactions of Kr in the metastable state were studied using the transitions at $\lambda = 0.8929 \mu\text{m}$ ($5p[1/2]_1 - 5s[3/2]_2$).

2. Experiment

The experiments (see also [6]) were performed by using a Tandem pulsed laser system with a cold-cathode electron gun [10]. The ~ 250 -keV pulsed electron beam of cross section $5 \times 100 \text{ cm}$ with a bell-shaped current pulse of base duration $\sim 2.5 \mu\text{s}$ was directed into a measuring chamber of active volume $5 \times 5 \times 100 \text{ cm}$, perpendicular to its optical axis. The electron current density was 1.5 A cm^{-2} . The source of probe signal was a broadband ISI-1 pulsed light source emitting ~ 30 - μs pulses [Fig. 2, curve (B)]. At the output from the light source, radiation was collimated into a beam 5 cm in diameter and, after passing through the measuring chamber with the mixture under study and through the monochromator tuned to the studied wavelength λ , was recorded with a high-speed photodetector and a digital oscilloscope. Part of radiation was directed, bypassing the measuring chamber, to the second monochromator.

In the afterglow of the electron beam pulse, upon completion of the recombination and relaxation processes the

concentration of 5s states in question should be determined primarily by the processes of their decay in reactions (1)–(4) [6]

$$\frac{d[\text{Kr}^*]}{dt} = -k_1[\text{Kr}][\text{He}][\text{Kr}^*] - k_2[\text{He}]^2[\text{Kr}^*] - (k_3 + k_4m)[\text{He}][\text{Kr}^*] \quad (8)$$

with a rate

$$k_d = k_1[\text{Kr}][\text{He}] + k_2[\text{He}]^2 + (k_3 + k_4m)[\text{He}]. \quad (9)$$

Here, k_1 and k_2 are the rate constants of excimerisation in reactions (1) and (2), respectively; k_3 is the rate constant for two-particle relaxation (3); k_4 is the rate constant of the quenching reaction by impurities in reaction (4); and m is the relative content of impurities in the mixture. In this case, the time dependence of the populations of the states under study can be represented as an exponential:

$$[\text{Kr}^*](t) = N_0 \exp(-k_d t). \quad (10)$$

When the excited medium is probed by monochromatic radiation at the wavelength of the transition from a highly excited state to the state in question, the absorption coefficient k should be proportional to the concentration of atoms in this state:

$$k(t) \sim [\text{Kr}^*](t). \quad (11)$$

In our case, with the width of the input and output slits of the monochromator equal to $\sim 0.2 \text{ mm}$, providing a satisfactory signal-to-noise ratio in the measurement path, the width of the instrumental function of the monochromator in the pressure range 1.75 to 4.0 atm considerably exceeds the linewidth of the observed optical transition. In this situation, the Bouguer–Lambert–Beer law, generally speaking, is not valid, and one needs to use the empirical, or so-called modified, form of the Bouguer–Lambert–Beer law [11, 12], relating the measured transmittance T with the absorption coefficient k by the expression

$$\ln(1/T) = (kL)^\gamma. \quad (12)$$

Here, L is the length of the absorbing medium excited by the electron beam and γ is a dimensionless factor that depends on the ratio of the widths of the absorption line and the instrumental function of the monochromator. The study of the experimental dependences

$$\ln \ln[1/T(L)] = \text{const} + \gamma \ln L \quad (13)$$

confirmed the applicability of the modified Bouguer–Lambert–Beer law and allowed us to determine the dimensionless factor γ , equal to 0.5, in our experimental conditions (see [13]).

It follows from expression (12) taking into account relations (11) and from the expected time dependence $[\text{Kr}^*](t)$ that the trailing edge of the ‘absorption pulse’ $\ln(1/T)$ should be purely exponential:

$$\ln[1/T(t)] \sim \exp(-\gamma k_d t). \quad (14)$$

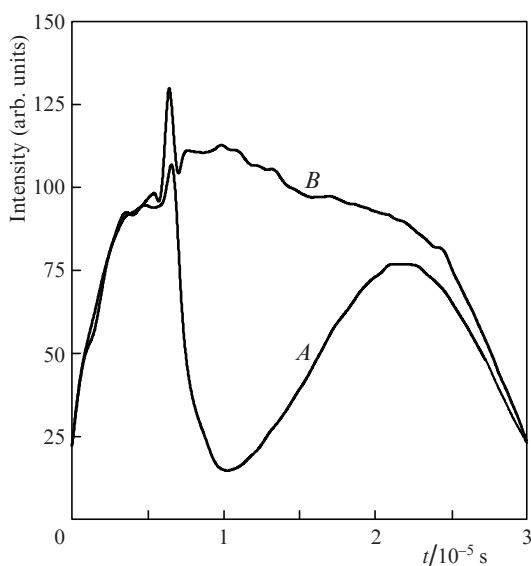


Figure 2. Time dependence of the intensity of the $0.8777\text{-}\mu\text{m}$ probe pulse transmitted through (A) and around (B) the excited volume (for the He:Kr = 100:1 mixture at a pressure 3.25 atm).

Taking the logarithm of expression (14) leads to the following time dependence of transmittance T in the afterglow:

$$\ln \ln[1/T(t)] = \text{const} - \gamma k_d t. \quad (15)$$

Figure 2 shows typical probe pulse oscillograms of the ISI-1 source, obtained for the He:Kr = 100:1 mixture at a pressure of 3.25 atm at the wavelength of the $5p[5/2]_2 - 5s[3/2]_1^o$ transition. By comparing the amplitudes of the signals at the input (B) and output (A) of the excited active medium, we can determine at each instant of time the transmittance T of the medium at the wavelength in question. Figure 3 presents the time dependence of the 'absorption pulse' $\ln(1/T)$ in the excited He–Kr mixture obtained from the oscillograms in Fig. 2.

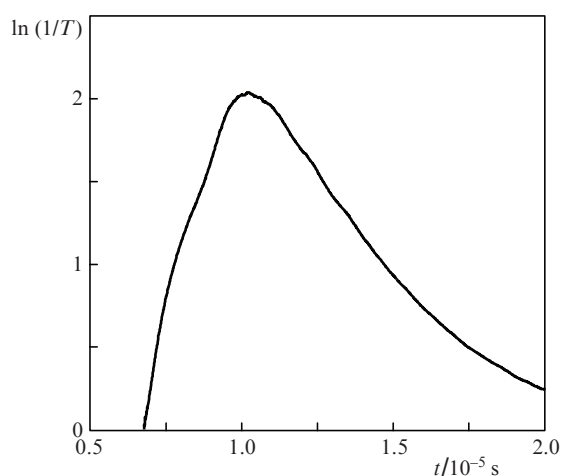


Figure 3. Time dependence of the absorption pulse $\ln(1/T)$ for probe pulses from Fig. 2.

Figure 4 shows the time dependence of the function $\ln \ln(1/T)$ for the trailing edge of the 'absorption pulse', corresponding to the oscillograms in Fig. 2. One can see that the approximation of this dependence by the linear function of type

$$\ln \ln(1/T) = r - \gamma k_d t \quad (16)$$

[curve (A)] does not lead to satisfactory results. This is explained by the fact [3, 4, 6] that due to the small collision quenching rates of the levels under study, it is necessary to take into account the influence of even weak recombination fluxes, which continue to populate the level in question in the afterglow (after the end of the electron pump pulse). In the experiment, the influence of the recombination effect noticeably differs from the exponential time dependence of the trailing edges of the 'absorption pulse' $\ln(1/T)$ in Fig. 3 and, therefore, demonstrates the nonlinear time dependence of $\ln \ln(1/T)$ (Fig. 4), which is different from (16).

To find the exponential component of the trailing edge of the absorption pulse, the time dependences were processed numerically using the approximation of curves in Fig. 4 by a quadratic polynomial

$$\ln \ln(1/T) = r - (\gamma g)^2(t - t_0)^2 - \gamma k_d(t - t_0), \quad (17)$$

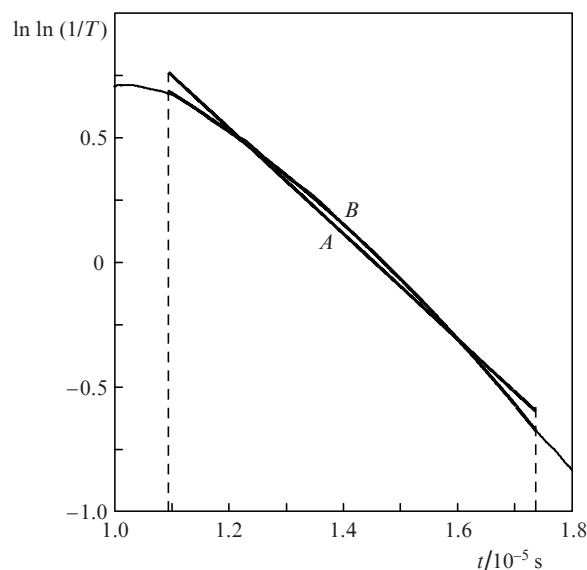


Figure 4. Time dependence of the function $\ln \ln(1/T)$, corresponding to the probe pulses in Fig. 2, approximated by (thick lines) the straight line (A) and the second-order curve (B).

where r , g , k_d are the approximation parameters and the time t_0 is measured from the end of the pump pulse. The linear part in (17) determines the required parameter k_d (collisional quenching rate of the level under study), while the small quadratic correction is related to the population dynamics of the level.

The quenching rates from the experimental time dependences $\ln \ln(1/T)$ were calculated with the help of the least squares method with varying the parameters r , g and k_d by using the Levenberg–Marquardt algorithm [14]. A set of the experimental data for the mixtures He:Kr = 25:1, 50:1 and 100:1 was processed at pressures from 1.75 to 4.0 atm with a step of 0.25 atm.

In the coordinates of Fig. 3 function (17) corresponds to the function

$$\ln(1/T) = \exp r \exp[-(\gamma g)^2(t - t_0)^2] \exp[-\gamma k_d(t - t_0)], \quad (18)$$

which is a superposition of the exponential describing the collisional quenching processes and the Gaussian pre-exponential giving a correction for recombination and relaxation processes. Determination of the real form of the pre-exponential in the analytical form is hardly possible because of the variety and complexity of its reactions, depending, in particular, on the time-varying temperature and density of the secondary electrons. However, in practice such a 'mnemonic' description in the dynamic range of variations in the transmittance, $T = 0.1 - 0.9$ (see Fig. 2) gives satisfactory results. For example, for each He–Kr mixture Fig. 5 presents the dependences of $k_d[\text{He}]^{-1}$, i.e., the quenching rate reduced to the concentration of He, on the concentration of this buffer gas. In this case, according to the linear dependences

$$k_d[\text{He}]^{-1} = (\delta k_1 + k_2)[\text{He}] + (k_3 + k_4 m) \quad (19)$$

which follows from (9) ($\delta = [\text{Kr}]/[\text{He}]$ is the relative content of krypton in the mixture), the experimental points with good accuracy lie on the straight lines originating from a common point on the ordinate axis, which indicates the adequacy of

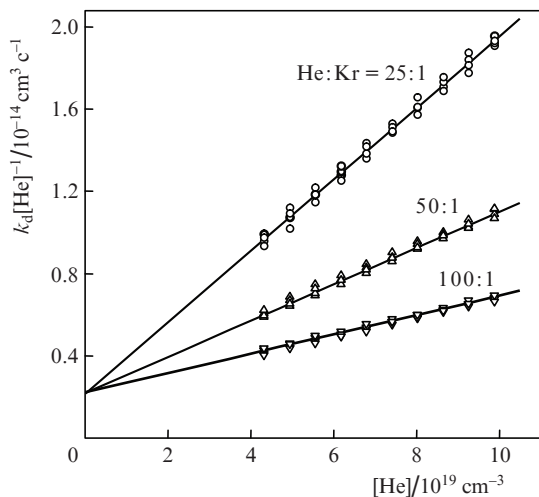


Figure 5. Dependences of the reduced quenching rates $k_d[\text{He}]^{-1}$ on the helium concentration in different He–Kr mixtures.

representation (18) and the correctness of the procedure of experimental data processing.

The thus obtained set of experimental values of $k_d^i([\text{Kr}], [\text{He}])$ was used to determine the rate constants of plasma-chemical reactions (1), (2), (5), (6) and the upper bound (up to an unknown value k_{4m}) of the rates of reactions (3) and (7). The values of the rate constants k_1 , k_2 , k_3 and k_5 , k_6 , k_7 (Tables 1 and 2) for the resonance and metastable levels, respectively, were calculated by the least-squares method with the use of the Levenberg–Marquardt algorithm by varying the sought-for constants in relations

$$k_d^i = k_{1(5)}[\text{Kr}][\text{He}] + k_{2(6)}[\text{He}]^2 + k_{3(7)}[\text{He}] \quad (20)$$

simultaneously for the entire set of the experimental values of k_d^i . The essence of the procedure was to construct in the coordinates $([\text{Kr}], [\text{He}])$ a curved surface

$$S([\text{Kr}], [\text{He}]) = k_{1(5)}[\text{Kr}][\text{He}] + k_{2(6)}[\text{He}]^2 + k_{3(7)}[\text{He}], \quad (21)$$

having the smallest deviation, in terms of the method, from the set of the experimental points [5].

Note that the processing of the experimental dependence of $\ln \ln[1/T(t)]$ with the use of a simple linear approximation (16) shows that this representation is badly suited for the experimental situation. Calculations performed allowed us to determine the rate constants of reactions (1), (5) and (3), (7) with very limited accuracy, which makes it possible to interpret them only as an upper bound k_1^{upp} , k_3^{upp} (Table 1) and k_5^{upp} , k_7^{upp} (Table 2). However, these calculations make it impossible to find quantitative values for the rate constants of reactions (2) and (6).

The results obtained in the present study (see also [6]) show that under our experimental conditions, the collisional quenching of $5s$ states of the Kr atom in the He–Kr mixture occurs during tree-particle reactions with the formation of a homonuclear dimer Kr_2^* (1) and during two-particle reactions (3) and (4). At the same time, the three-particle reaction (2) with the formation of a heteronuclear dimer HeKr^* is not involved in the collisional quenching of Kr^* . The latter circumstance may be explained by the fact that the heteronuclear dimer obtained in reaction (2) is unstable due to its low binding energy [15], and rapidly decays into the initial components in inverse collision reactions. In this case, the measured effective rate constant of the HeKr^* dimer formation is close to zero.

3. Conclusions

We have studied for the first time the processes of quenching of the resonance $\text{Kr}(5s[3/2]_1^0)$ state in He–Kr mixtures, which are similar in composition and pressure to the mixtures used in excimer lasers and high-pressure lasers on atomic transitions in inert gases. It has been shown that the main quenching channels of this state are the processes of excimerisation with the formation of a Kr_2^* dimer with a rate constant of $4.21 \times 10^{-33} \text{ cm}^6 \text{ s}^{-1}$ and buffer gas quenching with a rate constant of $2.21 \times 10^{-15} \text{ cm}^3 \text{ s}^{-1}$. At the same time, reactions with the formation of heteronuclear dimers virtually play no noticeable role.

We have refined the rate constants of similar reactions for the metastable $5s[3/2]_2^0$ level, which within the measurement accuracy correspond to the values obtained by us for the first time in paper [6].

Acknowledgements. The authors thank N.N. Ustinovskii for cooperation and useful discussions.

Table 1. Upper bounds k_i^{upp} and measured reaction rate constants k_i of the collisional quenching of the Kr atom in the $5s[3/2]_1^0$ state for the He–Kr mixture.

Reaction	k_i^{upp}	k_i	References
(1)	$5.3 \times 10^{-33} \text{ cm}^6 \text{ s}^{-1}$	$(4.21 \pm 0.42) \times 10^{-33} \text{ cm}^6 \text{ s}^{-1}$	This paper
(2)	–	$(4.5 \pm 1.2) \times 10^{-36} \text{ cm}^6 \text{ s}^{-1}$	This paper
(3)	$5.6 \times 10^{-15} \text{ cm}^3 \text{ s}^{-1}$	$(2.21 \pm 0.22) \times 10^{-15} \text{ cm}^3 \text{ s}^{-1}$	This paper

Table 2. Same as in Table 1 for the $5s[3/2]_1^0$ stste.

Reaction	k_i^{upp}	k_i	References
(5)	$3.1 \times 10^{-33} \text{ cm}^6 \text{ s}^{-1}$	$(2.88 \pm 0.29) \times 10^{-33} \text{ cm}^6 \text{ s}^{-1}$	[6]
	$3.8 \times 10^{-33} \text{ cm}^6 \text{ s}^{-1}$	$(2.88 \pm 0.29) \times 10^{-33} \text{ cm}^6 \text{ s}^{-1}$	This paper
(6)	–	$(4.6 \pm 1.3) \times 10^{-36} \text{ cm}^6 \text{ s}^{-1}$	[6]
	–	$(4.5 \pm 0.9) \times 10^{-36} \text{ cm}^6 \text{ s}^{-1}$	This paper
(7)	$4.7 \times 10^{-15} \text{ cm}^3 \text{ s}^{-1}$	$(1.51 \pm 0.15) \times 10^{-15} \text{ cm}^3 \text{ s}^{-1}$	[6]
	$2.7 \times 10^{-15} \text{ cm}^3 \text{ s}^{-1}$	$(1.55 \pm 0.16) \times 10^{-15} \text{ cm}^3 \text{ s}^{-1}$	This paper

References

1. Zayarnyi D.A., Kholin I.V. *Kvantovaya Elektron.*, **33** (6), 474 (2003) [*Quantum Electron.*, **33** (6), 474 (2003)].
2. Semenova L.V., Ustinovskii N.N., Kholin I.V. *Kvantovaya Elektron.*, **34** (3), 189 (2004) [*Quantum Electron.*, **34** (3), 189 (2004)].
3. Zayarnyi D.A., L'dov A.Yu., Kholin I.V. *Kvantovaya Elektron.*, **39** (9), 821 (2009) [*Quantum Electron.*, **39** (9), 821 (2009)].
4. Zayarnyi D.A., L'dov A.Yu., Kholin I.V. *Kvantovaya Elektron.*, **40** (2), 144 (2010) [*Quantum Electron.*, **40** (2), 144 (2010)].
5. Zayarnyi D.A., L'dov A.Yu., Kholin I.V. *Kvantovaya Elektron.*, **41** (2), 128 (2011) [*Quantum Electron.*, **41** (2), 128 (2011)].
6. Zayarnyi D.A., L'dov A.Yu., Kholin I.V. *Kvantovaya Elektron.*, **43** (8), 720 (2013) [*Quantum Electron.*, **43** (8), 720 (2013)].
7. Kholin I.V. *Kvantovaya Elektron.*, **33** (2), 129 (2003) [*Quantum Electron.*, **33** (2), 129 (2003)].
8. Dudin A.Yu., Zayarnyi D.A., Semenova L.V., Ustinovskii N.N., Kholin I.V., Chugunov A.Yu. *Kvantovaya Elektron.*, **18** (8), 921 (1991) [*Sov. J. Quantum Electron.*, **21** (8), 833 (1991)].
9. Zvereva G.N., Lomaev M.I., Rybka D.V., Tarasenko V.F. *Opt. Spektrosk.*, **102** (1), 36 (2007).
10. Zayarnyi D.A., L'dov A.Yu., Ustinovskii N.N., Kholin I.V. *Prib. Tekh. Eksp.*, (4), 102 (2010).
11. Oka T. *Res. Rep. Nagaoka Thsh. Coll.*, **13** (4), 207 (1977).
12. Davis C.C., McFarlane R.A. *J. Quant. Spectrosc. Radiat. Transfer*, **18**, 151 (1977).
13. Zayarnyi D.A., Kholin I.V., Chugunov A.Yu. *Kvantovaya Elektron.*, **22** (3), 233 (1995) [*Quantum Electron.*, **25** (3), 217 (1995)].
14. Demidenko E.Z. *Optimizatsiya i regressiya* (Optimisation and Regression) (Moscow: Nauka, 1989).
15. Nowak G., Fricke J. *J. Phys. B: At. Mol. Phys.*, **18**, 1355 (1985).